Temporal coherence and spectral linewidth of an injection-seeded transient collisional soft x-ray laser

L.M. Meng, D. Alessi, O. Guilbaud, Y. Wang, M. Berrill, B.M. Luther, S.R. Domingue, D.H. Martz, Denis Joyeux, Sébastien de Rossi, et al.

Temporal coherence and spectral linewidth of an injection-seeded transient collisional soft x-ray laser

L. M. Meng,[1,*] D. Alessi,[2] O. Guilbaud,[3] Y. Wang,[2] M. Berrill,[2] B.M. Luther,[2] S. R. Domingue,[2] D. H. Martz,[2] D. Joyeux,[4] S. De Rossi,[4] J. J. Rocca,[2] and A. Klisnick[1]

[1]*ISMO, Bât. 350, CNRS, Université Paris-Sud 11, 91405 Orsay, France*
[2]*NSF Center for EUV Science and Technology, Colorado State University, Fort Collins, CO, USA*
[3]*LPGP, Bât. 210, CNRS, Université Paris-Sud 11, 91405 Orsay, France*
[4]*LCFIO, Institut d'Optique-Graduate School, 91128 Palaiseau, France*
**limin.meng@u-psud.fr*

Abstract: The temporal coherence of an injection-seeded transient 18.9 nm molybdenum soft x-ray laser was measured using a wavefront division interferometer and compared to model simulations. The seeded laser is found to have a coherence time similar to that of the unseeded amplifier, ~1ps, but a significantly larger degree of temporal coherence. The measured coherence time for the unseeded amplifier is only a small fraction of the pulsewidth, while in the case of the seeded laser it approaches full temporal coherence. The measurements confirm that the bandwidth of the solid target amplifiers is significantly wider than that of soft x-ray lasers that use gaseous targets, an advantage for the development of sub-picosecond soft x-ray lasers.

OCIS codes: (140.7240) UV, XUV, and X-ray lasers; (300.6300) Spectroscopy, fourier transforms; (300.6560) Spectroscopy, x-ray.

References and links

1. Y. Wang, E. Granados, M. A. Larotonda, M. Berrill, B. M. Luther, D. Patel, C. S. Menoni, and J. J. Rocca, "High-brightness injection-seeded soft-x-ray-laser amplifier using a solid target," Phys. Rev. Lett. **97**(12), 123901 (2006).
2. Ph. Zeitoun, G. Faivre, S. Sebban, T. Mocek, A. Hallou, M. Fajardo, D. Aubert, Ph. Balcou, F. Burgy, D. Douillet, S. Kazamias, G. De Lachèze-Murel, T. Lefrou, S. Le Pape, P. Mercère, H. Merdji, A. S. Morlens, J. P. Rousseau, and C. Valentin, "A high-intensity highly coherent soft X-ray femtosecond laser seeded by a high harmonic beam," Nature **431**(7007), 426–429 (2004).
3. Y. Wang, E. Granados, F. Pedaci, D. Alessi, B. Luther, M. Berrill, and J. J. Rocca, "Phase-coherent, injection-seeded, table-top soft-X-ray lasers at 18.9 nm and 13.9 nm," Nat. Photonics **2**(2), 94–98 (2008).
4. J. Ph. Goddet, S. Sebban, J. Gautier, Ph. Zeitoun, C. Valentin, F. Tissandier, T. Marchenko, G. Lambert, M. Ribières, D. Douillet, T. Lefrou, G. Iaquaniello, F. Burgy, G. Maynard, B. Cros, B. Robillard, T. Mocek, J. Nejdl, M. Kozlova, and K. Jakubczak, "Aberration-free laser beam in the soft x-ray range," Opt. Lett. **34**(16), 2438–2440 (2009).
5. Y. Wang, M. Berrill, F. Pedaci, M. Shakya, S. Gilbertson, Z. Chang, E. Granados, B. Luther, M. Larotonda, and J. Rocca, "Measurement of 1-ps soft-x-ray laser pulses from an injection-seeded plasma amplifier," Phys. Rev. A **79**(2), 023810 (2009).
6. D. S. Whittaker, M. Fajardo, Ph. Zeitoun, J. Gautier, E. Oliva, S. Sebban, and P. Velarde, "Producing ultrashort, ultraintense plasma-based soft-x-ray laser pulses by high-harmonic seeding," Phys. Rev. A **81**(4), 043836 (2010).
7. A. Klisnick, O. Guilbaud, D. Ros, K. Cassou, S. Kazamias, G. Jamelot, J. C. Lagron, D. Joyeux, D. Phalippou, Y. Lechantre, M. Edwards, P. Mistry, and G. J. Tallents, "Experimental study of the temporal coherence and spectral profile of the 13.9nm transient X-ray laser," JQRST **99**, 370 (2006).
8. O. Guilbaud, F. Tissandier, J.-P. Goddet, M. Ribière, S. Sebban, J. Gautier, D. Joyeux, D. Ros, K. Cassou, S. Kazamias, A. Klisnick, J. Habib, P. Zeitoun, D. Benredjem, T. Mocek, J. Nedjl, S. de Rossi, G. Maynard, B. Cros, A. Boudaa, and A. Calisti, "Fourier-limited seeded soft x-ray laser pulse," Opt. Lett. **35**(9), 1326–1328 (2010).

#145253 - $15.00 USD Received 15 Apr 2011; revised 25 May 2011; accepted 25 May 2011; published 7 Jun 2011

9. F. Tissandier, S. Sebban, M. Ribière, J. Gautier, Ph. Zeitoun, G. Lambert, A. Barszczak Sardinha, J.-P. Goddet, F. Burgy, T. Lefrou, C. Valentin, A. Rousse, O. Guilbaud, A. Klisnick, J. Nejdl, T. Mocek, and G. Maynard, "Observation of spectral gain narrowing in a high-order harmonic seeded soft-x-ray amplifier," Phys. Rev. A **81**(6), 063833 (2010).
10. M. Berrill, D. Alessi, Y. Wang, S. R. Domingue, D. H. Martz, B. M. Luther, Y. Liu, and J. J. Rocca, "Improved beam characteristics of solid-target soft x-ray laser amplifiers by injection seeding with high harmonic pulses," Opt. Lett. **35**(14), 2317–2319 (2010).
11. R. Keenan, J. Dunn, P. K. Patel, D. F. Price, R. F. Smith, and V. N. Shlyaptsev, "High-repetition-rate grazing-incidence pumped x-ray laser operating at 18.9 nm," Phys. Rev. Lett. **94**(10), 103901 (2005).
12. B. M. Luther, Y. Wang, M. A. Larotonda, D. Alessi, M. Berrill, M. C. Marconi, J. J. Rocca, and V. N. Shlyaptsev, "Saturated high-repetition-rate 18.9-nm tabletop laser in nickellike molybdenum," Opt. Lett. **30**(2), 165–167 (2005).
13. O. Guilbaud, A. Klisnick, K. Cassou, S. Kazamias, D. Ros, G. Jamelot, D. Joyeux, and D. Phalippou, "Origin of microstructures in picosecond X-ray laser beams," Europhys. Lett. **74**(5), 823–829 (2006).
14. O. Guilbaud, A. Klisnick, D. Joyeux, D. Benredjem, K. Cassou, S. Kazamias, D. Ros, D. Phalippou, G. Jamelot, and C. Möller, "Longitudinal coherence and spectral profile of a nickel-like silver transient soft X-ray laser," Eur. Phys. J. D **40**(1), 125–132 (2006).
15. M. Born, and E. Wolf, "*Principles of Optics*" 7th edition, (Cambridge University Press, 2002), Chap. 10.8.3.
16. R. F. Smith, J. Dunn, J. R. Hunter, J. Nilsen, S. Hubert, S. Jacquemot, C. Remond, R. Marmoret, M. Fajardo, P. Zeitoun, L. Vanbostal, C. L. S. Lewis, M.-F. Ravet, and F. Delmotte, "Longitudinal coherence measurements of a transient collisional x-ray laser," Opt. Lett. **28**(22), 2261–2263 (2003).
17. O. Larroche, D. Ros, A. Klisnick, A. Sureau, C. Möller, and H. Guennou, "Maxwell-Bloch modeling of x-ray-laser-signal buildup in single- and double-pass configurations," Phys. Rev. A **62**(4), 043815 (2000).
18. M. A. Larotonda, Y. Wang, M. Berrill, B. M. Luther, J. J. Rocca, M. M. Shakya, S. Gilbertson, and Z. Chang, "Pulse duration measurements of grazing-incidence-pumped high repetition rate Ni-like Ag and Cd transient soft x-ray lasers," Opt. Lett. **31**(20), 3043–3045 (2006).

The demonstration of injection-seeded soft X-ray lasers (SXRL), generated by either transient collisional excitation in solid target plasmas [1] or optical-field-ionization in gaseous targets [2], has opened new prospects for the utilization of high-brightness plasma-based coherent soft x-ray sources for various applications. The use of high-order harmonic (HH) pulses as a seed has led to a dramatic enhancement of the spatial coherence [3,4] over those exhibited in amplified spontaneous emission (ASE) operation. The degree of temporal coherence is an important parameter that also needs to be characterized for applications. The coherence time, linked to the spectral width $\Delta\nu$ of the laser line through $\tau_c \sim 1/\Delta\nu$, also determines the ultimate minimum pulse duration that can be achieved. The shortest pulse duration measured to date for a seeded SXRL is ~1.1 ps in a Ne-like Ti plasma [5]. In order to make further progress towards sub-picosecond pulse soft x-ray lasers [5,6] it is important to obtain experimental information about the spectral characteristics of these sources. This is a challenging measurement because the narrow linewidth of SXRL lines (typically $\Delta\lambda/\lambda \sim 10^{-5}$) typically lies beyond the resolution limit of existing spectrometers in this spectral range.

In this paper we report the first measurement of the temporal coherence and spectral width of a transient solid-target SXRL injection-seeded by HH pulses. Measurements for a seeded 18.9 nm Ni-like Mo amplifier were compared to results for the ASE mode of operation and model simulations. It is shown that the injection-seeded and ASE lasers have a similar linewidth, but that the degree of temporal coherence of the seeded laser is significantly larger, approaching full temporal coherence. The narrow linewidth was resolved using a wavefront-division interferometer specifically designed to measure temporal coherence [7] from which the spectral linewidth is inferred. Such interferometer was previously used to investigate other types of SXRLs, including a 32.8 nm injection-seeded optical-field-ionization (OFI) SXRL in a Xe gas medium developed at Laboratoire d'Optique Appliquée (France) [8,9]. The transient amplifiers created by irradiation of solid targets [10] studied here are measured to have significantly larger linewidths that support the generation of shorter pulse durations.

#145253 - $15.00 USD Received 15 Apr 2011; revised 25 May 2011; accepted 25 May 2011; published 7 Jun 2011

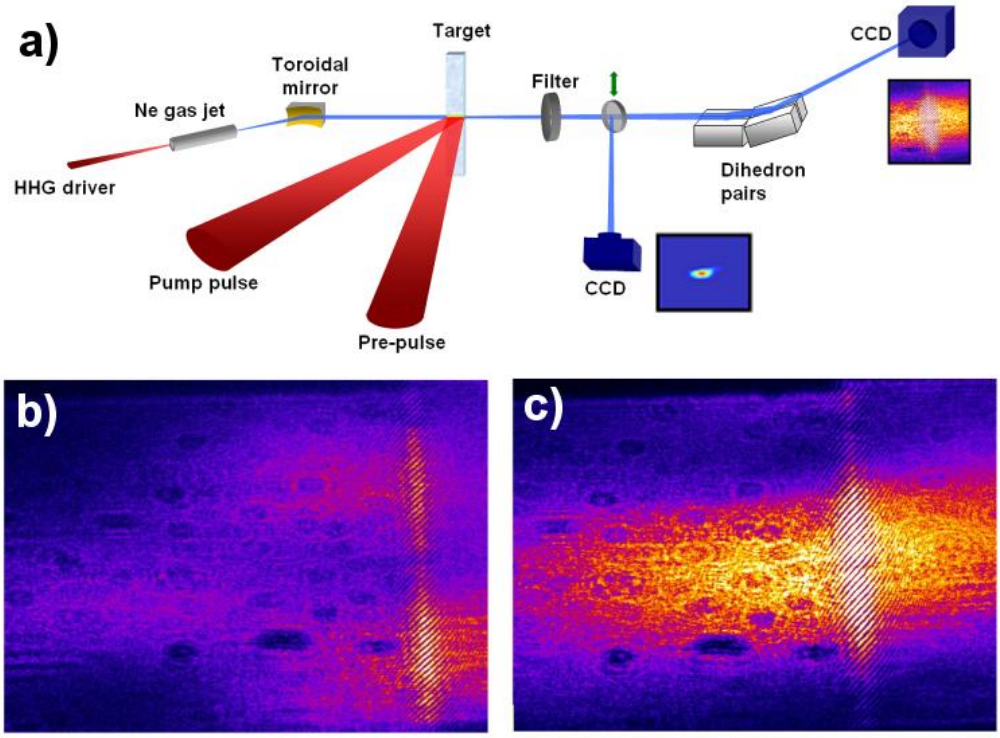

Fig. 1. (a) Experimental set up used to measure the temporal coherence of an 18.9 nm molybdenum plasma amplifier. Interferograms of the ASE (b) and seeded (c) 18.9 nm laser beam with a zero path difference between the arms of the interferometer. A 300 nm thick aluminum filter was used. In the ASE case (b) the beam is composed of several juxtaposed speckle structures. Two of them are apparent (orange white zones) in the fringe area. In the seeded case (c) one single spot is apparent, corresponding to the amplified seed beam.

The experiment was carried out at Colorado State University (CSU) using a 18.9 nm SXRL amplifier in the transient regime generated by irradiation of a solid molybdenum slab target at grazing incidence [11, 12] with pulses from an λ = 800 nm Titanium:Sapphire (Ti:Sa) laser. A sequence of two 210 ps FWHM duration pulses with energies of 45 mJ and 420 mJ are focused onto a 30 µm wide by 4 mm long line at normal incidence to the target producing a plasma with a large fraction of the ions in the Ni-like state. At a delay of 500 ps, a 3.3 ps FWHM duration heating pulse of 1J energy impinges onto the plasma at a grazing incidence angle of 23 degrees in an overlapping line focus, resulting in transient population inversion at 18.9nm. This laser amplifier was seeded with the 43rd harmonic of a femtosecond pulse from a Ti:Sa laser as described in [3] yielding a highly collimated, almost fully spatially coherent beam. The duration of the Ti:Sa pulses used to generate the high harmonic seed in this experiment was ~100fs. The output characteristics of the seeded laser are similar to that described in [3]. The SXRL beam was directed toward a variable path-difference interferometer which was set at a distance of 3 m from the source (Fig. 1(a)). A far-field monitor, consisting of a 45 degrees multilayer mirror and an XUV CCD camera could be inserted in the X-ray laser beamline (see Fig. 1(a)) to allow verification of the beam alignment before each series of measurements. The interferometer consists of a pair of dihedrons slightly tilted towards each other and irradiated under 6 degrees grazing incidence [7]. Interference fringes, which are formed in the overlapping region, are detected with a XUV CCD camera. The CCD chip is inclined to a 35 degrees incidence angle in order to increase the apparent fringe spacing to ~5 pixels/fringe. A variable path difference between the two interfering

#145253 - $15.00 USD Received 15 Apr 2011; revised 25 May 2011; accepted 25 May 2011; published 7 Jun 2011

beamlets is introduced by translating one of the two dihedrons vertically. Using a dihedron instead of a flat mirror ensures that the loss of fringe visibility when the path difference is increased is solely due to the finite temporal coherence, not to a geometrical change in the beam overlap, which depends also of the finite spatial coherence of the source. The tilt angle between the interfering mirrors is 1.6 mrad, leading to an interference field of 1 mm in the plane normal to the beam, or 1.8 mm in the CCD detector plane.

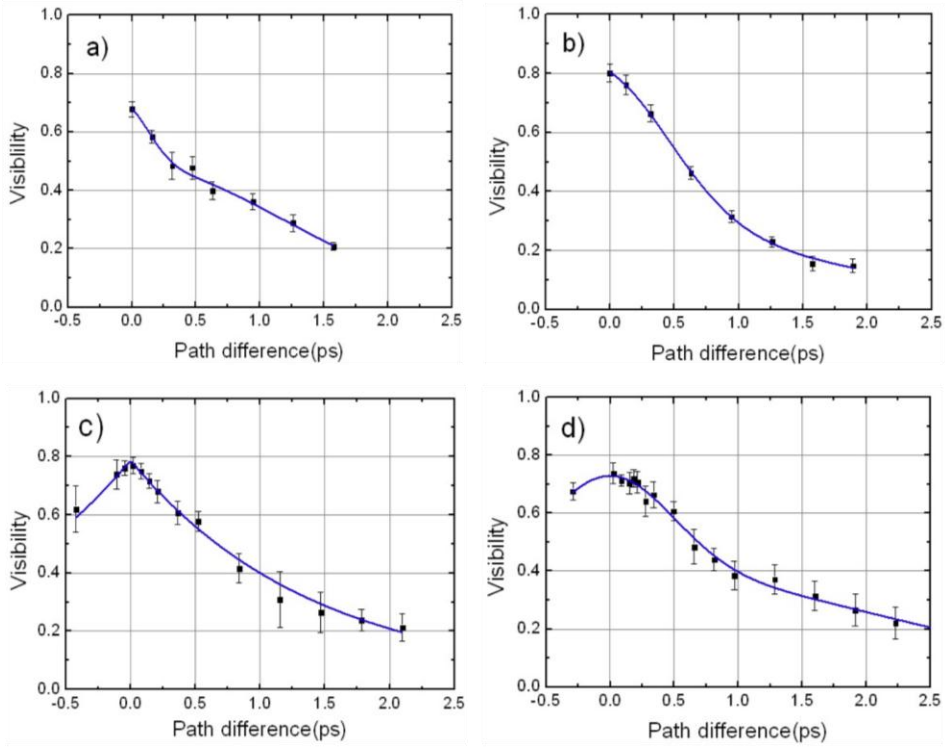

Fig. 2. (a) Visibility as a function of the path difference measured in the injection-seeded mode for the plasma amplifier lengths of 2 mm (a), 3 mm (b) and 4 mm (c). (d) Visibility data corresponding to the 4 mm ASE amplifier. The solid-line curves show the best analytical fit of the experimental data. Different types of analytical functions were used: (a) sum of two Gaussians; (b) sum of Gaussian and decreasing exponential; (c) decreasing exponential; (d) sum of two Gaussians

Series of interferograms with increasing path difference were acquired for different X-ray laser amplifier lengths. Figure 1 (b, c) shows two typical interferograms of the 18.9 nm laser obtained in the ASE mode and injection seeded mode respectively. In the ASE case, the beam is composed of randomly distributed speckles [13] which are apparent in the image. In the injection seeded case, the highly-collimated amplified HH beamlet is centered on the interference region [10]. Each interferogram was processed numerically to infer the fringe visibility for a given path difference. After background subtraction, a Fourier-transform with a sliding window [8] was applied to the full interference zone, yielding a map of visibility. The visibility was found to vary by about 20% across the zone of interest in the ASE case. This variation can be attributed to the non-uniformity of the X-ray laser beam [14] which can be seen in the images shown in Fig. 1. When the two non-uniform beamlets overlap, the visibility of the fringes is maximum only at those positions where the intensities in the two interferometer arms are equal and it is lower elsewhere. Hence the maximum visibility in the interference field was considered as the relevant value for a given interferogram. For the injection seeded case, the visibility was measured in a restricted zone containing the amplified

#145253 - $15.00 USD Received 15 Apr 2011; revised 25 May 2011; accepted 25 May 2011; published 7 Jun 2011

HH beamlet, excluding the ASE zone. In this restricted zone the variation of visibility is smaller than in the ASE case, namely less than 10%.

Figure 2 (a-c) shows the measured visibility curves obtained from the path difference scans for three different injection seeded Mo amplifier lengths. Figure 2(d) shows the measured visibility curve corresponding to the 18.9 nm laser amplifier (L = 4 mm) operated in the ASE mode. Each data point is the average of the visibility measured over 5 to 10 laser shots, and the error bar represents the standard deviation, mainly due to shot-to-shot fluctuation. In each graph, the solid-line curve shows the best analytical fit of the experimental data. To infer the coherence time τ_C and the corresponding frequency linewidth $\Delta\nu$ from our measurements we used the definitions given in [15], assuming that the spectral profile is symmetrical with respect to the central frequency $\bar{\nu}$:

$$\tau_c^{\,2} = \frac{\int_0^\infty t^2 \cdot \left|V^2(t)\right| \cdot dt}{\int_0^\infty \left|V^2(t)\right| \cdot dt} \qquad \Delta\nu^2 = 2\frac{\int_0^\infty \upsilon^2 \cdot \left|G^2(\nu+\bar{\nu})\right| \cdot d\nu}{\int_0^\infty \left|G^2(\nu+\bar{\nu})\right| \cdot d\nu} \qquad (1)$$

where *V(t)* is the visibility as a function of the path difference (given by the analytical fit), *G(ν)* is the spectral power density and $\bar{\nu}$ is the average central frequency of the line. *G(ν)* is given by the Fourier-transform of *V(t)*. The above definitions, which are based on the quadratic mean of the quantities, are less sensitive to the shape of the visibility curve (i.e. to the chosen fit for the experimental data) than the usual definitions used previously [9, 14, 16]. Hence it can be judged as more appropriate in cases like ours where the shape of the visibility curve is difficult to determine accurately.

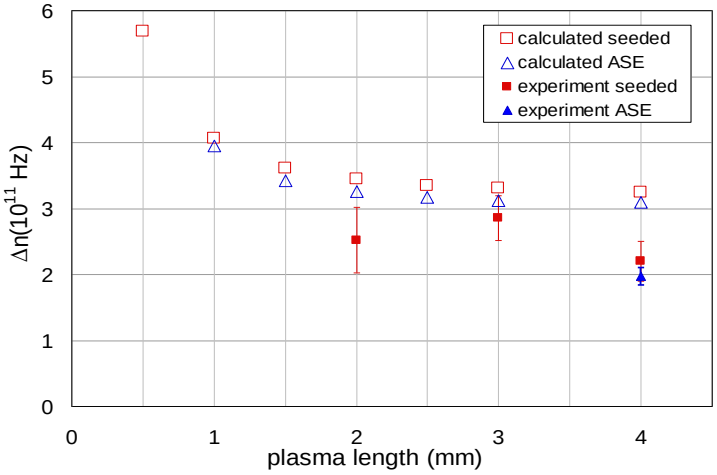

Fig. 3. Measured and computed linewidth (as defined in Eq. (1) of the injection-seeded and ASE 18.9 nm molybdenum SXRLs for different plasma lengths (see color online).

The variation of the linewidth of the seeded and ASE lasers as a function of amplifier length was simulated using the combination of a 2-dimensional hydrodynamic/atomic physics code and a 3-dimensional ray propagation code developed at CSU. The ray propagation tracks the amplification for each frequency component as the individual rays propagate taking into account refraction and gain saturation [10]. While this code does not allow the full self-consistent treatment of Maxwell-Bloch codes [17], it does include temporal broadening due to bandwidth narrowing and has the advantage of including a more detailed atomic model. The code was previously shown to satisfactorily predict the physical behavior as well as the pulse duration and energy of injection-seeded transient soft x-ray lasers in agreement with experiments [3,5]. The evolution of the plasma parameters was computed by the

#145253 - $15.00 USD Received 15 Apr 2011; revised 25 May 2011; accepted 25 May 2011; published 7 Jun 2011

hydrodynamic code and fed into the ray propagation code. The ray propagation calculation is fully resolved in space, angle, frequency, and time. Figure 3 displays the values of the measured and simulated quadratic linewidth of the injection-seeded and ASE lasers for different plasma lengths obtained using the expression defined in (1). It can be observed that smaller spectral linewidth (2.2×10^{11} Hz) corresponding to the larger temporal coherence time, (1.0 ± 0.2) ps is obtained for the longest plasma length of 4 mm, as expected from amplified radiation in the absence of saturation rebroadening. However, since most of the line narrowing due to amplification occurs in the first 2 mm of the plasma column, the measured variations as a function of plasma length are small and mostly within the error bars. It is also observed that the linewidth of the ASE X-ray laser, 1.95×10^{11} Hz, is slightly smaller (although again within the error bars) than the injection-seeded laser linewidth corresponding to the same amplifier length, as already observed for the 32.8 nm OFI SXRL in a recent experiment [9]. Such a behavior is consistent with the numerical simulations, and reflects the fact that the linewidth of the ASE and seeded lasers are dominated by the bandwidth of the amplifier, that is in turn dependent of the plasma conditions. There is no line rebroadening after saturation. The measured longitudinal coherence time for the longer seeded columns lengths of 3 and 4 mm are 0.8 ps and 1.0 ps respectively. These values are similar to the measured pulse duration of 1.13 ± 0.47 ps for a seeded solid target Ne-like Ti laser [5], that our model computations predict to be close to the pulse duration of the seeded Ni-like Mo laser, 1.3-1.5 ps. In contrast, the measured temporal coherence time is much shorter than the 4-6 ps duration computed for the ASE Ni-like Mo laser, that in turn resembles the measured ~5ps pulse durations of other similar transient collisional grazing incidence ASE lasers that were accurately predicted using the same model [18]. Therefore, it is concluded that while the injection-seeded and ASE lasers are measured to have very similar linewidths, the seeded laser has a significantly higher degree of temporal coherence that approaches full temporal coherence. The coherent time of the injection-seeded Ni-like Mo laser is also several times shorter than the transform limited pulsewidth of 4.7 ps reported for the 32.9 nm OFI laser [8], corroborating the high potential of injection-seeded transient collisional solid target amplifiers for the development of table-top SXRLs of shorter pulse duration.

Acknowledgments

This work was supported by the NSF Center for Extreme Ultraviolet Science and Technology under NSF Award EEC-0310717, by the Chemical Sciences, Geosciences and Biosciences Division, Office of Basic Energy Sciences, U.S. Department of Energy.

#145253 - $15.00 USD Received 15 Apr 2011; revised 25 May 2011; accepted 25 May 2011; published 7 Jun 2011